UCRL-19804 c.2
UC-28 Particle
Accelerator and High
Voltage Machines
(TID-4500 55th Ed.)

STUDY OF A MULTIELEMENT REGENERATIVE EXTRACTION SYSTEM FOR THE BERKELEY 184-INCH CYCLOTRON

Arthur C. Paul

May 1970

AEC Contract No. W-7405-eng-48

RECEIVED
LAWRENCE
RADIATION LABORATORY
SEP 30 1970
LIBRARY AND
DOCUMENTS SECTION

TWO-WEEK LOAN COPY

This is a Library Circulating Copy which may be borrowed for two weeks. For a personal retention copy, call Tech. Info. Division, Ext. 5545

LAWRENCE RADIATION LABORATORY
UNIVERSITY of CALIFORNIA BERKELEY

UCRL-19804 c.2

DISCLAIMER

This document was prepared as an account of work sponsored by the United States Government. While this document is believed to contain correct information, neither the United States Government nor any agency thereof, nor the Regents of the University of California, nor any of their employees, makes any warranty, express or implied, or assumes any legal responsibility for the accuracy, completeness, or usefulness of any information, apparatus, product, or process disclosed, or represents that its use would not infringe privately owned rights. Reference herein to any specific commercial product, process, or service by its trade name, trademark, manufacturer, or otherwise, does not necessarily constitute or imply its endorsement, recommendation, or favoring by the United States Government or any agency thereof, or the Regents of the University of California. The views and opinions of authors expressed herein do not necessarily state or reflect those of the United States Government or any agency thereof or the Regents of the University of California.

STUDY OF A MULTIELEMENT REGENERATIVE EXTRACTION SYSTEM FOR THE BERKELEY 184-INCH CYCLOTRON*

Arthur C. Paul

Lawrence Radiation Laboratory
University of California
Berkeley, California 94720

May 1970

ABSTRACT

This paper discusses the matrix-method calculation of the properties of a three-element regenerative extraction system for a synchrocyclotron. It is shown that the three-element-system stability calculation can be conveniently parameterized in matrix formalism separating the perturbations strengths from the field geometry. Both linear and nonlinear perturbation can be employed with a computer code written to track particle vectors and calculate stability tables from the single-turn matrix for a multielement extraction system. The particle-tracking includes simulation of the effect of acceleration during regeneration. Several extraction systems are considered and comparison is made with the results of numerical integration of the exact equations of motion in the measured magnetic field of the 184-inch cyclotron.

INTRODUCTION

During the extraction-improvement studies for the Berkeley 184-inch synchrocyclotron we have considered three-element regenerative extraction systems. The motivation behind the three-element system has been to effect efficient radial extraction while preserving vertical stability for all turns through the regenerator. Two calculational methods have been used: exact integration of the equations of motion in the magnetic field[1] and the matrix method of LeCouteur[2]. This paper describes our work using the matrix method. In order to study the regenerative effect of these three-element systems, we have extended the standard two-element equations for the stability criteria in matrix formalism and show that a separation of the perturbation strength from the geometry (location of the perturbations) is possible.

The geometry of the extraction system considered in this report is shown in Fig. 1. The perturbations Q_1, Q_2, and Q_3 begin at radii r_1, r_2, and r_3 and are separated by angles α, β, and γ respectively. These perturbations are considered superimposed on the normal weak focusing field of the cyclotron.

The effect of field perturbations on regeneration is studied by calculating the matrices for the several field regions comprising a turn. The single turn product matrix can be used to track a given particle vector one or more turns, or provide information on stability from the value of the trace of the matrix.[3] The matrix transforms a particle vector $\binom{x}{x}$ where $x' = dx/d\theta$, θ being the azimuth formed by the right

handed polar coordinate system (x, z, θ). We define the field index describing the field fall-off as

$$n = -\frac{dB}{dR}\frac{\rho}{B_0} ,$$

where ρ is the radius of curvature, PC/eB_z, for a particle of momentum P in field B_z on the median plane. The perturbations produced by a peeler, regenerator, or additional extraction elements is represented by a matrix which produces a deflection of the particle without displacing the trajectory

$$\begin{pmatrix} x \\ x' \end{pmatrix} = \begin{pmatrix} 1 & 0 \\ -Q_j & 1 \end{pmatrix} \begin{pmatrix} x_0 \\ x_0' \end{pmatrix}$$

$$\begin{pmatrix} z \\ z' \end{pmatrix} = \begin{pmatrix} 1 & 0 \\ Q_j & 1 \end{pmatrix} \begin{pmatrix} z_0 \\ z_0' \end{pmatrix} .$$

Here Q_j is the strength of the jth perturbation of width $\Delta\theta_j$, $Q_j = -n_j\Delta\theta_j$. Note that Q has the sign of the field gradient:

$$P(Q_j) = \begin{pmatrix} 1 & 0 \\ -Q_j & 1 \end{pmatrix} .$$

The effect of the weak focusing cyclotron field of azimuthal extent α_j is given by the following matrix:

$$A(\alpha_j) = \begin{pmatrix} \cos \nu\alpha_j & \frac{1}{\nu}\sin \nu\alpha_j \\ -\nu \sin \nu\alpha_j & \cos \nu\alpha_j \end{pmatrix} ,$$

where $\nu = \sqrt{n}$ for vertical motion and $\nu = \sqrt{1-n}$ for radial motion. A complete revolution about the cyclotron is simulated by the product of the matrices in the order encountered:

$$A(2\pi) = A(\gamma)\, P(Q_3)\, A(\beta)\, P(Q_2)\, A(\alpha)\, P(Q_1).$$

This single turn matrix represents the effect of the three perturbations Q_1, Q_2, and Q_3 separated by angles α, β, and γ in the cyclotron (Fig. 1). Radial or vertical stability requires that the trace of the matrix be less than 2. Calculating the trace, we obtain:

$$\begin{aligned}
\text{Trace } A(2\pi) = {} & 2 \cos \nu\alpha \cos \nu\beta \cos \nu\gamma \\
& - 2 \sin \nu\alpha \sin \nu\beta \cos \nu\gamma \\
& - 2 \cos \nu\alpha \sin \nu\beta \sin \nu\gamma \\
& - 2 \sin \nu\alpha \cos \nu\beta \sin \nu\gamma \\
& + Q_1 (\tfrac{1}{\nu} \sin \nu\alpha \cos \nu\beta \cos \nu\gamma \\
& + \tfrac{1}{\nu} \cos \nu\alpha \sin \nu\beta \cos \nu\gamma \\
& - \tfrac{1}{\nu} \sin \nu\alpha \sin \nu\beta \sin \nu\gamma \\
& + \tfrac{1}{\nu} \cos \nu\alpha \cos \nu\beta \sin \nu\gamma) \\
& + Q_2 (\tfrac{1}{\nu} \cos \nu\alpha \sin \nu\beta \cos \nu\gamma \\
& + \tfrac{1}{\nu} \cos \nu\alpha \cos \nu\beta \sin \nu\gamma \\
& - \tfrac{1}{\nu} \sin \nu\alpha \sin \nu\beta \sin \nu\gamma \\
& + \tfrac{1}{\nu} \sin \nu\alpha \cos \nu\beta \cos \nu\gamma) \\
& + Q_3 (\tfrac{1}{\nu} \cos \nu\alpha \cos \nu\beta \sin \nu\gamma \\
& - \tfrac{1}{\nu} \sin \nu\alpha \sin \nu\beta \sin \nu\gamma \\
& + \tfrac{1}{\nu} \sin \nu\alpha \cos \nu\beta \cos \nu\gamma \\
& + \tfrac{1}{\nu} \cos \nu\alpha \sin \nu\beta \cos \nu\gamma) \\
& + Q_1Q_2(\tfrac{1}{\nu^2} \sin \nu\alpha \sin \nu\beta \cos \nu\gamma \\
& + \tfrac{1}{\nu^2} \cos \nu\alpha \sin \nu\beta \sin \nu\gamma) \\
& + Q_1Q_3 (\tfrac{1}{\nu^2} \sin \nu\alpha \cos \nu\beta \sin \nu\gamma \\
& + \tfrac{1}{\nu^2} \cos \nu\alpha \sin \nu\beta \sin \nu\gamma) \\
& + Q_2Q_3 (\tfrac{1}{\nu^2} \cos \nu\alpha \sin \nu\beta \sin \nu\gamma \\
& + \tfrac{1}{\nu^2} \sin \nu\alpha \sin \nu\beta \cos \nu\gamma) \\
& + Q_1Q_2Q_3 (\tfrac{1}{\nu^3} \sin \nu\alpha \sin \nu\beta \sin \nu\gamma).
\end{aligned}$$

Considerable insight into this horrendous expression can be obtained by decomposing the trace into the sum of vector elements W_j obtained by the matrix product of a perturbation matrix, P, and a geometry vector, G.

$$\text{Trace } A(2\pi) = \sum_j W_j ,$$

$$W_j = \sum_k P_{jk}\, G_k ,$$

$$P = \begin{bmatrix}
2 & 0 & 0 & 0 & 0 & -2\nu^2 & -2\nu^2 & -2\nu^2 \\
0 & -Q_1 & -Q_1 & -Q_1 & Q_1 & 0 & 0 & 0 \\
0 & -Q_2 & -Q_2 & -Q_2 & Q_2 & 0 & 0 & 0 \\
0 & -Q_3 & -Q_3 & -Q_3 & Q_3 & 0 & 0 & 0 \\
0 & 0 & 0 & 0 & 0 & 0 & Q_1Q_2 & Q_1Q_2 \\
0 & 0 & 0 & 0 & 0 & Q_1Q_3 & 0 & Q_1Q_3 \\
0 & 0 & 0 & 0 & 0 & Q_2Q_3 & Q_2Q_3 & 0 \\
0 & 0 & 0 & 0 & \frac{-Q_1Q_2Q_3}{\nu} & 0 & 0 & 0
\end{bmatrix} ,$$

$$G \equiv \begin{bmatrix} \cos \nu\alpha \cos \nu\beta \cos \nu\gamma \\ \cos \nu\alpha \sin \nu\beta \cos \nu\gamma/\nu \\ \cos \nu\alpha \cos \nu\beta \sin \nu\gamma/\nu \\ \sin \nu\alpha \cos \nu\beta \cos \nu\gamma/\nu \\ \sin \nu\alpha \sin \nu\beta \sin \nu\gamma/\nu \\ \cos \nu\alpha \sin \nu\beta \cos \nu\gamma/\nu^2 \\ \sin \nu\alpha \sin \nu\beta \cos \nu\gamma/\nu^2 \\ \sin \nu\alpha \cos \nu\beta \sin \nu\gamma/\nu^2 \end{bmatrix} .$$

The geometry vector G depends on the azimuthal location of the perturbations and the weak focusing strength of the cyclotron field while the perturbation strengths enter in an 8×8 matrix of simple structure. The advantage of this representation is that for a given geometry, the effect of change in perturbation strengths can be readily evaluated.

If we consider the usual two element system made of perturbations Q_1 and Q_2 separated by angles α and β, we obtain, after elimination of zero elements:

$$W = \begin{bmatrix} 2 & 0 & 0 & -2\nu^2 \\ 0 & -Q_1 & -Q_1 & 0 \\ 0 & -Q_2 & -Q_2 & 0 \\ 0 & 0 & 0 & Q_1Q_2 \end{bmatrix} \begin{bmatrix} \cos \nu\alpha \cos \nu\beta \\ \cos \nu\alpha \sin \nu\beta/\nu \\ \sin \nu\alpha \cos \nu\beta/\nu \\ \sin \nu\alpha \sin \nu\beta/\nu^2 \end{bmatrix} .$$

This gives the usual expression for the trace of a regenerator-peeler system[4]:

$$\text{Trace} = 2 \cos \nu(\alpha+\beta) - \frac{1}{\nu}(Q_1+Q_2)\sin(\alpha+\beta) + \frac{Q_1Q_2}{\nu} \sin \nu\alpha \sin \nu\beta$$

Here Q_1 and Q_2 are positive for a rising field and negative for a falling field. From the field of the 184-inch cyclotron, Fig. 2, we have $Q_1 = -0.4$, $Q_2 = 0.6$, $\nu_r = 0.98$, $\nu_Z = 0.2$, $\alpha = 90$ deg and $\beta = 270$ deg giving:

$$W_r = \begin{pmatrix} 1.984 \\ -.05116 \\ .07673 \\ .2486 \end{pmatrix} = \begin{pmatrix} 2 & 0 & 0 & -1.9208 \\ 0 & +.4 & .4 & 0 \\ 0 & -.6 & -.6 & 0 \\ 0 & 0 & 0 & -.24 \end{pmatrix} \begin{pmatrix} -.00296 \\ -.09598 \\ -.03191 \\ -1.0361 \end{pmatrix}$$

$$W_z = \begin{pmatrix} .6180 \\ -1.902 \\ 2.853 \\ -1.500 \end{pmatrix} = \begin{pmatrix} 2 & 0 & 0 & -0.080 \\ 0 & -.4 & -.4 & 0 \\ 0 & .6 & .6 & 0 \\ 0 & 0 & 0 & -.24 \end{pmatrix} \begin{pmatrix} .5590 \\ .90818 \\ 3.8471 \\ 6.250 \end{pmatrix}$$

The radical trace is $\sum_j W_{rj} = 2.258$ and the vertical trace is $\sum_j W_{zj} = 0.0691$, this then gives regeneration without vertical instability.

Given T_R, the desired value of the trace of the radial matrix, and the strength of one regenerator and peeler, say T_r, Q_1 and Q_3, the value of Q_2 required to produce T_r can be calculated from the expression

$$L = 2\nu_r^2 (g_6+g_7+g_8)$$

$$K = g_2+g_3+g_4-g_5$$

$$Q_2 = \frac{Tr - 2g_1 + L + (Q_1+Q_3)K - Q_1Q_3(g_6+g_8)}{K + Q_1(g_7+g_8) - Q_3(g_6+g_7) + Q_1Q_3g_5\nu_r^{-1}} .$$

where g_j are the elements of the geometry vector G evaluated with $\nu = \nu_r = \sqrt{1-n}$. The trace in the vertical plane produced by this value of Q_2 is obtained from

$$\begin{aligned} T_z = {} & 2h_1 - 2\nu_z(h_6+h_7+h_8) \\ & - (h_2+h_3+h_4-h_5)(Q_1+Q_2+Q_3) \\ & + Q_1Q_2(h_7+h_8) + Q_1Q_3(h_6+h_8) \\ & + Q_2Q_3(h_6+h_7) - Q_1Q_2Q_3h_5\nu_z^{-2} , \end{aligned}$$

where h_j are the elements of the geometry vector G evaluated with $\nu = \nu_z = \sqrt{n}$. This equation simplifies to a straight line when plotting T_z vs. Q_2 (Fig. 3):

$$T_z = a + bQ_2 ,$$

$$\begin{aligned} a = {} & 2h_1 - 2\nu_z(h_6+h_7+h_8) \\ & - (h_2+h_3+h_4-h_5)(Q_1+Q_3) + Q_1Q_3(h_6+h_8) , \\ b = {} & Q_3(h_6+h_7) + Q_1(h_7+h_8) \\ & - (h_2+h_3+h_4-h_5)(Q_1+Q_3) - Q_1Q_3Q_5\nu_z^{-2} . \end{aligned}$$

In order to be able to calculate extraction properties for machines which consist of a more complicated sequence of regions than provided by the three Courant-Synder matrices AM, BM, and CM provision is made to calculate the AM, BM, and CM matrices from an unlimited number of submatrices when using

the 16. element of the computer code REGEN.[5] Each submatrix is defined by the angle of bend ζ, the field index n, the perturbation strengh Q, and spiral angle λ. The submatrices have the form

$$\begin{pmatrix} \cos \nu\zeta & \frac{1}{\nu} \sin \nu\zeta \\ -\nu \sin\nu\zeta + Q \tan\lambda & \cos \nu\zeta \end{pmatrix},$$

where $\nu = \sqrt{n}$ for vertical motion or equals $\sqrt{1-n}$ for horizontal motion and Q has opposite sign in the two planes. These submatrices take the form of wedge-focusing matrices when $\zeta = 0$,

$$\begin{pmatrix} 1 & 0 \\ \pm Q \tan\lambda & 1 \end{pmatrix},$$

and the form of the Courant-Synder matrix when $Q = 0$, $\zeta \neq 0$:

$$\begin{pmatrix} \cos \nu\zeta & \frac{1}{\nu} \sin \nu\zeta \\ -\nu \sin \nu\zeta & \cos \nu\zeta \end{pmatrix}.$$

When n is negative or greater than 1 the sin and cos are replaced by their hyperbolic counterpart for vertical and horizontal motion respectively.

It is evident that an extraction system of four or more elements can be studied by burying these elements into the AM, BM, or CM matrix by the use of a 16. element.

TRACKING OF PARTICLES

Modification must be made to the matrices if particle vectors are to be tracked in the presence of acceleration. The effect of acceleration is to increase the radius r_{eq} of the reference trajectory by a small amount da brought about by the increased rigidity of the particles with increased energy. A particle enters the jth perturbation of strength Q_j if its radius, $r = r_{eq} + x$ exceeds the starting radius of the perturbation, r_j. If r is less than r_j, the perturbation has no effect and is represented by a unit transformation. The angular deflection produced by a linear perturbation is given by the amount of penetration into the perturbation:

$$x' = x_0' \qquad r_{eq} + x < r_j,$$

$$x' = x_0' + (r_{eq} + x - r_j)\, Q_j \qquad r_{eq} + x \geq r_j.$$

If the perturbation is linear, Q_j is constant; if the perturbation is nonlinear, $Q_j = f(r_{eq} + x - r_j)$. This may be represented by defining the third row of the particle vector to be $dr = r_{eq} - r_j$, the difference between the equilibrium orbit radius and the starting radius of the perturbation:

$$\begin{pmatrix} x \\ x' \\ d_r \end{pmatrix} = \begin{pmatrix} 1 & 0 & 0 \\ -Q & 1 & -Q \\ 0 & 0 & 0 \end{pmatrix} \begin{pmatrix} x_0 \\ x_0' \\ d_r \end{pmatrix}$$

$$\begin{pmatrix} z \\ z' \\ 0 \end{pmatrix} = \begin{pmatrix} 1 & 0 & 0 \\ Q & 1 & 0 \\ 0 & 0 & 1 \end{pmatrix} \begin{pmatrix} z_0 \\ z_0' \\ 0 \end{pmatrix}$$

where $Q = 0$ if $r_{eq} + x < r_j$ and $Q = Q_j$ if $r_{eq} + x \geq r_j$. These matrices now will transform the particle vectors simulating acceleration. Particle vectors should be tracked in conjugate pairs $(0, x_0')$, $(x_0, 0)$ for $(z, 0)$, $(0, z_0')$ until either x, x' or z, z' are greater than some maximum value or until the radius is greater than some maximum radius, R_{max}, or the number of turns exceeds some predetermined maximum number.

MATRIX RESULTS FOR THE 184-INCH CYCLOTRON

Consider a particle starting with $x = x' = 0$ and equilibrium radius r_{eq} less than the starting radii of the peeler or regenerator, r_j. The particle vector $\binom{x}{x'}$ remains a null vector until the addition of da to the radius at each turn produced by acceleration brings the equilibrium radius up to r_j, then the vector $\binom{x}{x'}$ is excited by the matrix transformations. For the 184-inch cyclotron we choose a peeler strength of -0.4 and a regenerator strength of 0.6, (Fig. 2). Figures 4 and 5 show the results

of particle tracking with $Q_1 = -0.4$, $Q_2 = 0.6$, $Q_3 = 0$, $\alpha = 90$ deg, $\beta = 270$ deg, $\gamma = 0$, $V_r = 0.98$, and $V_z = 0.2$ in the radial and vertical betatron phase space. Figures 4 and 5 should be compared with similar figures obtained by numerical integration of the exact equations of motion in the measured magnetic field of the 184-inch cyclotron (Figs. 6 and 7). Departure of the figures from each other for the last two revolutions results from the actual nonlinear Q value shown in Fig. 2. Figure 8 shows the projection of Fig. 7 onto the real z axis. The vertical blow-up seen on turns N-1 and N, Fig. 8, can be understood by examining the motion of the particles in the vertical trace space, Fig. 9, as the regenerator Q_r and peeler strength Q_p vary over the values shown in Fig. 2 for n = 0.04, $\alpha = 90$ deg, $\beta = 270$ deg and $\gamma = 0$. No vertical growth is observed until turns N-1 and N, where the vertical trace becomes greater than 2 because of the larger peeler strength, Q_p, encountered on the last two turns where the radius values are 87.5 and 90.0 inches. The radial trace space is shown in Fig. 10, which shows that the last revolution does not contribute to regeneration since radial stability occurs.

VERTICAL FOCUSING LENS AT RADIAL NODE

We have examined the effect of placing a vertically focusing lens, Q_3, at the radial regeneration node. The vertical and radial trace spaces are shown in Fig. 11 as functions of lens strength for values of Q_1, Q_2, and n appropriate for the turn under consideration. For a zero lens strength we have the values of the vertical trace for the various turns calculated in the preceding section. As we change the lens strength the vertical trace can be made to increase or decrease in value for any given turn while maintaining radial instability, but nowhere is there a lens value for which the vertical trace is less than 2 for all turns. It then must be concluded that a vertical lens placed at the radial node cannot correct the vertical over-focusing produced by the peeler on turns N-1 and N.

MAGNETIC BUMP BEAM STRETCHER

As another example of the use of the computer code REGEN is the calculation of the stability diagram and regeneration properties of a gradient coil used to stretch the beam. This scheme[6] calls for the acceleration of the beam into a field region that off-centers the beam so as to prevent its entry into the regenerator. The acceleration is then turned off and extraction accomplished by a slow reduction of the magnetic bump, slowly bringing the beam into the regenerator, large radial amplitudes first. Figure 12 shows the stability diagram. The area marked "vertical instability" is the area for which the absolute value of the trace of the vertical matrix is greater than 2; the area marked "regeneration" is the area for which the radial trace is greater than 2 and the absolute value of the vertical trace is less than 2. The effect on the stable area for various values of the gradient coil Q_2 is indicated. This figure is obtained from the results of a three-dimensional map produced by varying the perturbations Q_1, Q_2, and Q_3 by the following data:

4.	90.	0.	270.	.98	.2
5.	3.	0.	.8	.2	
5.	2.	-2.	1.	.1	
5.	1.	-1.3	0.	.1	
1.	0.				

It will be noted that as the harmonic coil pushes the particles off center, out into the fringing field, the value of the strength of the fringe field increases (Fig. 2). When the orbits are out to about 85 in., $Q_1 = 0.6$, $Q_3 = 0$, and we have vertical instability (Fig. 12). The action of the field under acceleration can be investigated by accelerating out to a radius of 81.15 in. with the gradient bump Q_2 on:

3.	-.4	-.2	.6	81.2	78.	81.2	81.15
4.	90.	0.	270.	.98	.2		
1.	.1	.02	.1	.02	80.80	1.	

The particle transformation is stopped when $r = r_{eq} + x > R_{max} = 81.15$. The acceleration is turned off, R_{max} set to 100 in., and the vector transformation continued for an additional hundred turns:

9.	2.	0.
9.	4.	100.
10.	100.	

Regeneration does not occur, since the trace of the radial matrix is less than 2 with the perturbation on. This is effected by the off-centering of the orbits so that they do not enter the regenerator. The perturbation is now turned off and the vector transformation continued for an additional twenty turns:

3.	-.4	0.	.6
10.	20.		

However, now regeneration occurs and extraction is accomplished, since the peeler strength is -0.4 and the regenerator strength is 0.6.

DATA INPUT TO REGEN

All data input to program REGEN is in 8F10.0 format except for comments, which are in 8A10 format. The first number on a data input card specifies the type and is unique for the "type" of data that is being read on the card. A comment card must be preceded by a 13. card, otherwise data can be read-in in any order. Blank cards are ignored and may be used where desired in the data deck. Data cards are read in order until a 1. or 10. card is encountered, which causes the data structure so defined to be executed, after which the reading of data continues until another 1. or 10. card is encountered. A 20. data card terminates the job. The appendix shows the operating instruction generated by the code along with some sample data.

1. X. XP. Z. ZP. R. CONJ.

This data card specifies the particle or particles to be tracked in the previously defined matrix structure and initiates execution. If CONJ = 0, a particle is started in the radial and vertical phase space at coordinates (X, XP) and (Z, ZP) at a radius R. R is used to determine the degree of penetration into perturbations. If CONJ = 1, six conjugate particles are tracked with radial and vertical phase-space starting coordinates of (X, 0), (Z, 0), (0, ZP) and (0, XP), (Z, 0), (0, ZP).

2. reg. SW. d. g.

Several different perturbation types may be used at any of the regions Q_1, Q_2, and Q_3 of Fig. 1. The type of perturbation to be used at perturbation reg. is specified by the value of SW and is given in the following table. D is the distance over which the perturbation may be nonlinearly turned on to the final value specified by the type 3. data card. J = reg. = 1., 2., or 3. define $\lambda = (r_{eq} + x - r_j)/d$, then

SW	Name	$r_{eq} + x - r_j < d$	$0 < r_{eq} + x - r_j < d$	$d < r_{eq} + x - r_j$
1	Step function	0	Q_j	Q_j
2	Exponential	0	$Q_j(1-e^{\lambda})/(1-e)$	Q_j
3	Sine wave	0	$Q_j(\mathrm{SIN}\frac{\pi}{2}\lambda)$	Q_j
4	Linear	0	$Q_j(\lambda)$	Q_j
5	Quadratic	0	$Q_j(\lambda^2)$	Q_j
6	Cubic	0	$Q_j(\lambda^3)$	Q_j
7	Power	0	$Q_j(\lambda^g)$	Q_j

3. Q_1. Q_2. Q_3. r_1. r_2. r_3. r_{max}

The data card specifies the perturbation strengths and starting radii for the three perturbation regions. The values of the strengths Q are related to the field gradient by $Q_j = (dB/dR_j)(\rho/B_0)\Delta\theta_j$; r_{max} is the maximum radius that particles being tracked may obtain at the entrance to Q_1.

4. α. β. γ. ν_r. ν_Z.

This data card specifies the matrices to be used in transforming the particles through angles α, β, and γ in degrees, where α is the angle between Q_1 and Q_2, β is the angle between Q_2 and Q_3, and γ is the angle between Q_3 and Q_1; ν_r and ν_Z are the radial and vertical betatron frequencies respectively.

5. Region. Qmin. Qmax. Qstep.

This data card will cause the perturbation, Region, to be varied from Qmin to Qmax in Steps of Qstep where Region is 1., 2., or 3.

The radial and vertical trace of the transfer matrix will be calculated for each of the Q values generated and a table of trace values produced. One, two, or all three regions may be varied. The maximum number of values that the Q's can have assigned is 5000. If all three regions are to be varied then n = [(QAmax - QAmin)/QAstep + 1]. [(QBmax - QBmin)/QBstep + 1]. [(QCmax - QCmin)/QCstep + 1] $\leq$ 5000. The order of the 5. cards determines the order of variable in the table output. If the regions are designated as A, B, and C where A, B, C = 1, 2, or 3, then the data cards shown will produce the indicated table structure:

5.	A.	QAmax.	QAmin.	QAstep.
5.	B.	QBmax.	QBmin.	QBstep.
5.	C.	QCmax.	QCmin.	QCstep.
1.				

Each page of the table will be for a new value of variable A. Variable C will be horizontal across the page with a maximum of 14 points per page. If variable C has more than 14 values, then more than one page will be generated. Variable B will run vertically down the page with 53 points per page.

Variable A

Variable C . . . . . →

Variable B

↓

6. MN. R(1, 1). R(1, 2). R(1, 3). R(2, 1). R(2, 2). R(2, 3).

This data card allows for the numerical input of the transfer matrices AM(α), BM(β), and CM(γ). NM specifies which matrix and which plane is being read as follows: NM = 11 radial AM matrix, MN = 12 vertical AM matrix, NM = 21 radial BM matrix, NM = 22 vertical BM matrix, NM = 31 radial CM matrix, and NM = 32 vertical CM matrix.

7. CODE. VALUE.

This data card specifies the output options to be used.

CODE = 1. Value = orbit output step interval.
CODE = 2. Value = 1. Print matrix with the 5. element calculations.
Value = 0. Stop matrix output with 5. element calculations.
CODE = 3. Value = 1. Print matrix with vector tracking.
Value = 0. Stop matrix printing with vector tracking.
CODE = 4. Value = ν TEST.
CODE = 5. Page eject.

8. Xmax. XPmax. Zmax. ZPmax.

This data card specifies the maximum value that the betatron oscillations are allowed to obtain before the calculations are terminated.

9. CODE. VALUE.

This data card specifies input parameters to be used by the code.

CODE = 1. Value = maximum number of revolutions.

CODE = 2. Value = radial increment per revolution produced by acceleration.

CODE = 3. Value = starting radius of particles, REQ.

CODE = 4. Value = Rmax, maximum radius allowed at entrance to Q_1 perturbation before calculations are stopped.

10. N.

This data card allows the orbit calculations to be continued for an additional N revolutions without redefining the particle vectors.

11. N.

This data card specifies that the eigenvalues and eigenvectors of the transfer matrices should be calculated if N = 1., and not calculated if N = 0.

12. I. J. K.

This data card specifies that the matrices for each nonzero i. j, k region shall be read from binary tape, tape 8. The four horizontal elements 11, 12, 21, and 22 are read followed by the four vertical elements 11, 12, 21, and 22 for each region specified. The input data is assigned to matrix AM for i, j, or k = 1, to BM for i, j, or k = 2, and to CM for i, j, or k = 3; i.e., the data card 12. 2. 3. 1. reads the 8 elements for matrix BM, the 8 elements for matrix CM, and then the 8 elements for matrix AM, whereas the data card 12. 1. 0. 0. reads only the 8 elements for matrix AM.

13. N.

This data card must precede any comment or title cards in the data set and specifies that N such cards follow immediately.

14. 1.

This card restores the internal constants to their initial values:

r_0 = 82.	a = .002
r_1 = 0	Nmax = 100
r_2 = 0	Perturbation SW = 1
r_3 = 0	Perturbation d = 1
Q_1 = 0	JEIGEN = False
Q_2 = 0	Xmax = 8.
Q_3 = 0	XPmax = 8.
	Zmax = 4.
	ZPmax = 4.
	Rmax = 100000.
	Unit multipliers for 15. element set to unity.

15. CODE. VALUE.

This data card specifies a unit change for the matrices AM, BM, and CM.

CODE = 1. Value = multiplier of matrix element 11

CODE = 2. Value = multiplier of matrix element 12

CODE = 3. Value = multiplier of matrix element 13

CODE = 4. Value = multiplier of matrix element 21

CODE = 5. Value = multiplier of matrix element 22

CODE = 6. Value = multiplier of matrix element 23

16. Reg. N.

Alpha. K. Q. Beta.

Alpha. K. Q. Beta.

.

.

.

Alpha. K. Q. Beta. N such cards.

These data cards allow any or all of the matr ces AM, BM, or CM to be defined as the product of an unlimited number of submatrices defined by the angle of bend α, field index K, flutter Q, and spiral angle β. Reg = 1, 2, or 3 specifies region AM, BM, or CM. N is the number of submatrices into which the region is to be divided.

17. LABLE.

This data card causes the data following up to a 17. 0. data card to be stored in an array and tagged by the number lable. Lable can be any positive integral number greater than zero. A 14. element will be ignored by the 17. element. The data so stored can be executed by the use of the 18. element.

18. LABLE. N.

This data card causes the data named Lable stored by the 17. data card to be executed N times. Example: Calculate stability tables for several sets of auxiliary matrices read from tape 8.

```
17.  1.
12.  1.  2.  3.
 5.  1. -2.  0.  .1
 5.  2.  0.  1.  .1
 1.
17.  0.
18.  1.  5.
```

20.

Terminates calculations.

FOOTNOTES AND REFERENCES

*Work done under the auspices of the U. S. Atomic Energy Commission.

1. A. C. Paul, Study of the Regenerative Extraction of the Berkeley 184-Inch Synchrocyclotron, Lawrence Radiation Laboratory Report UCRL-18211 (1968).

2. J. K. LeCouteur, The Regenerative Deflector for Synchrocyclotrons, Proc. Phys. Soc. (London) B64, 1073 (1952).

3. E. D. Courant and H. S. Snyder, Theory of the Alternating-Gradient Synchrotron, Ann. Phys. 3, 1 (1958).

4. Compared with Eq. 17 of Ref. 2.

5. See section on Data Input to REGEN.

6. Suggested by Hogil Kim, Modification Studies for the Berkeley 184-Inch Cyclotron, by D. J. Clark, H. Kim, E. R. MacKenzie, and J. T. Vale, IEEE Transactions on Nuclear Science, NS-13, 235 (August 1966).

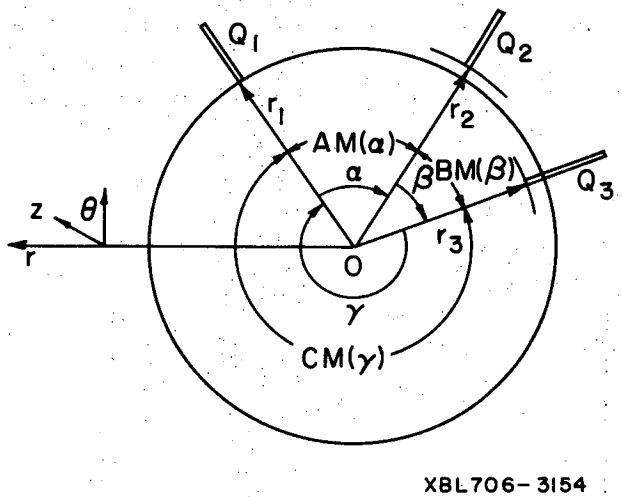

Fig. 1. Geometry of the three-region extraction system. The center of the cyclotron is at O. The perturbations Q_1, Q_2, Q_3 begin at radii r_1, r_2, and r_3 and are separated by angles α, β, and γ respectively. The matrices AM( ), BM( ) and CM( ) transform the particle vectors through the angles α, β, and γ.

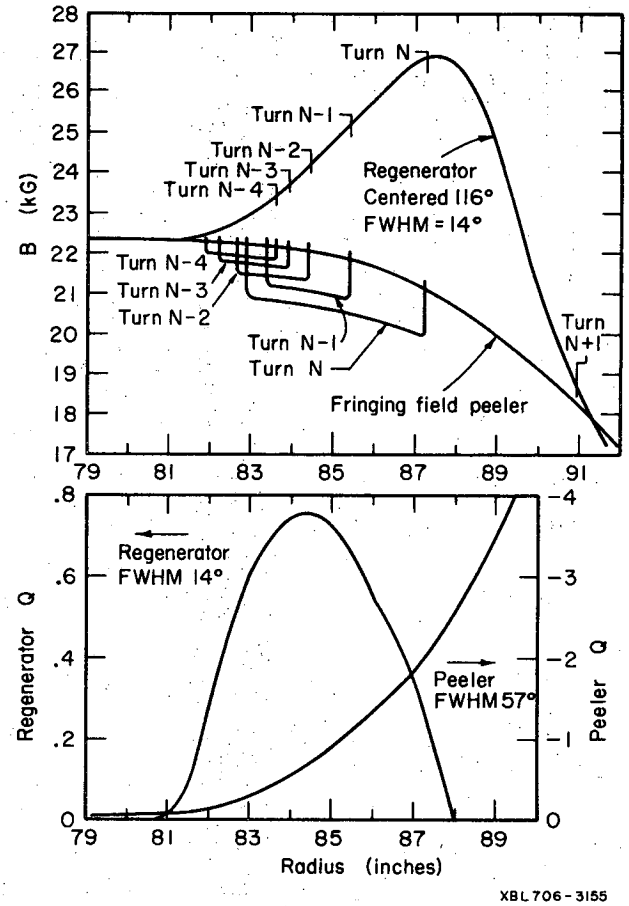

Fig. 2. Field and peeler-regenerator strengths for 184-inch cyclotron.

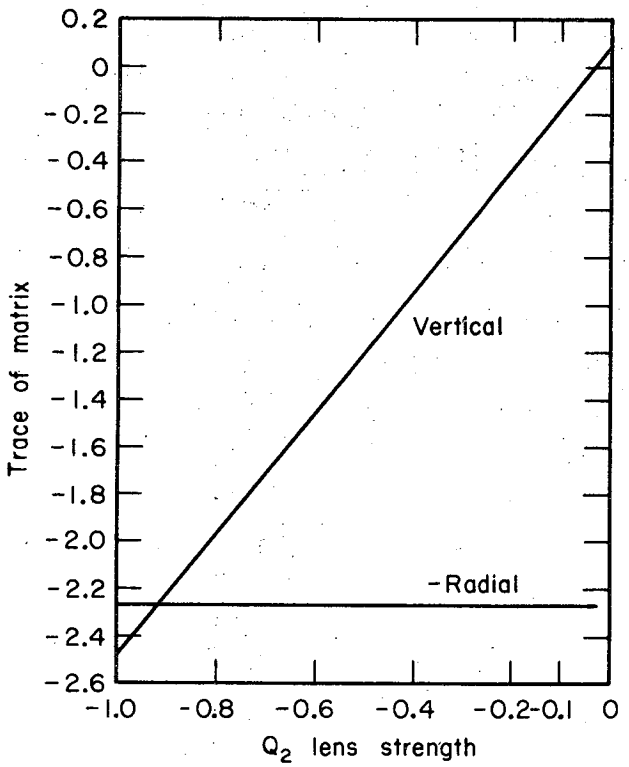

Fig. 3. Effect of lens placed at radial node. Here $\alpha = 40$ deg, $\beta = 230$ deg, $\gamma = 90$deg, $Q_1 = 0.6$, $Q_3 = -0.4$, and $n = 0.04$.

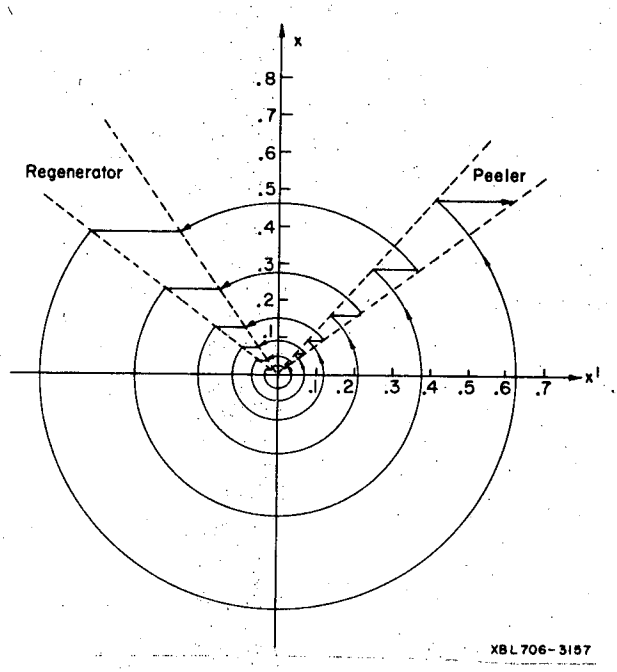

Fig. 4. Radial phase space motion during regeneration calculated from the single-turn matrix transformation of a null vector excited by acceleration into the extraction system.

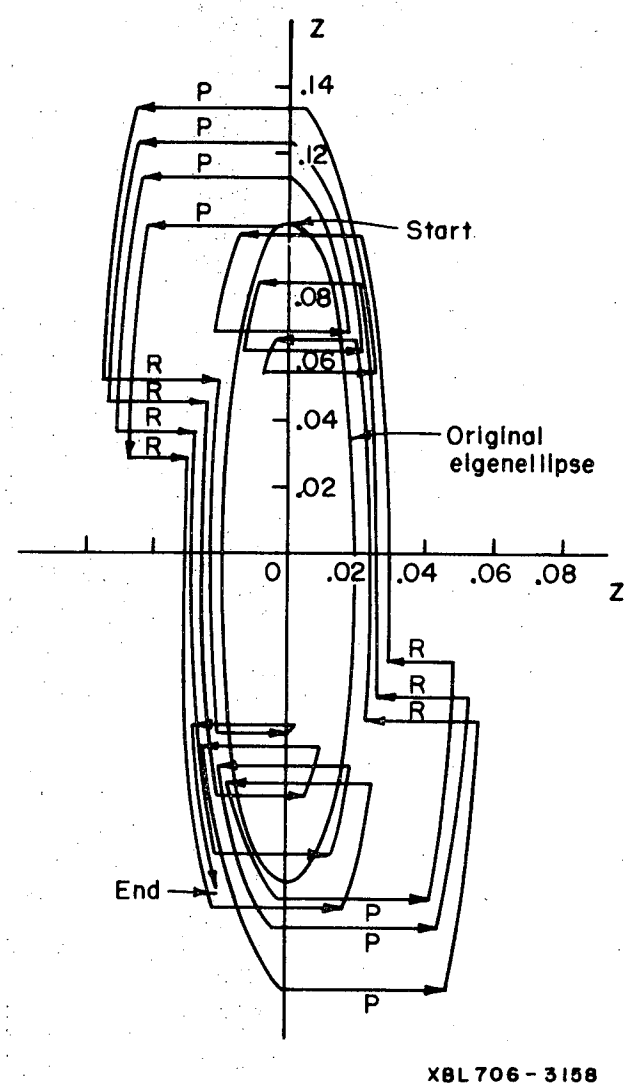

Fig. 5. Vertical phase space motion during regeneration calculated from single-turn matrix for the radial motion shown in Fig. 4.

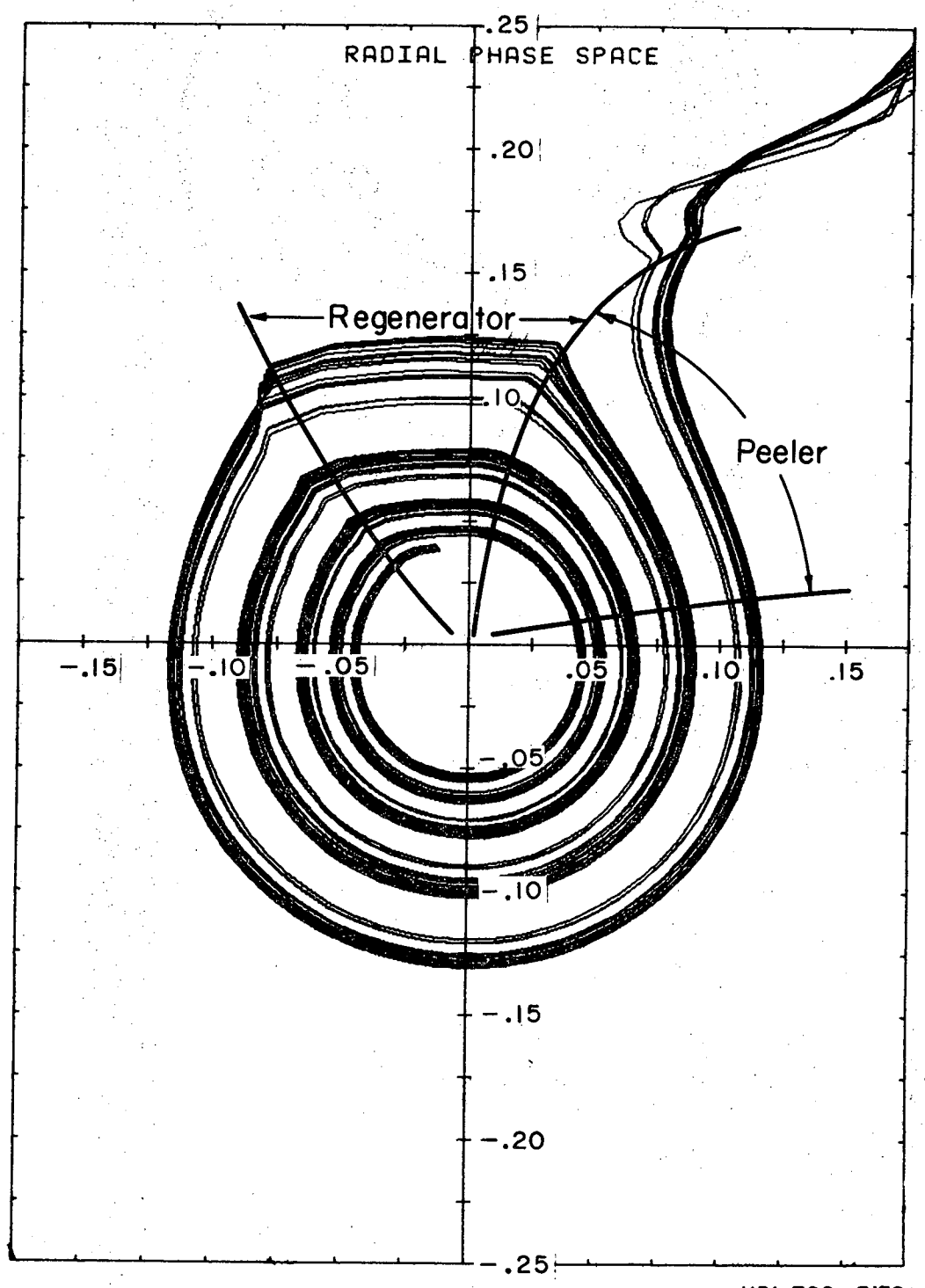

XBL 706-3159

Fig. 6. Radial phase space motion calculated by numerical integration of equations for motion in magnetic field of 184-inch cyclotron.

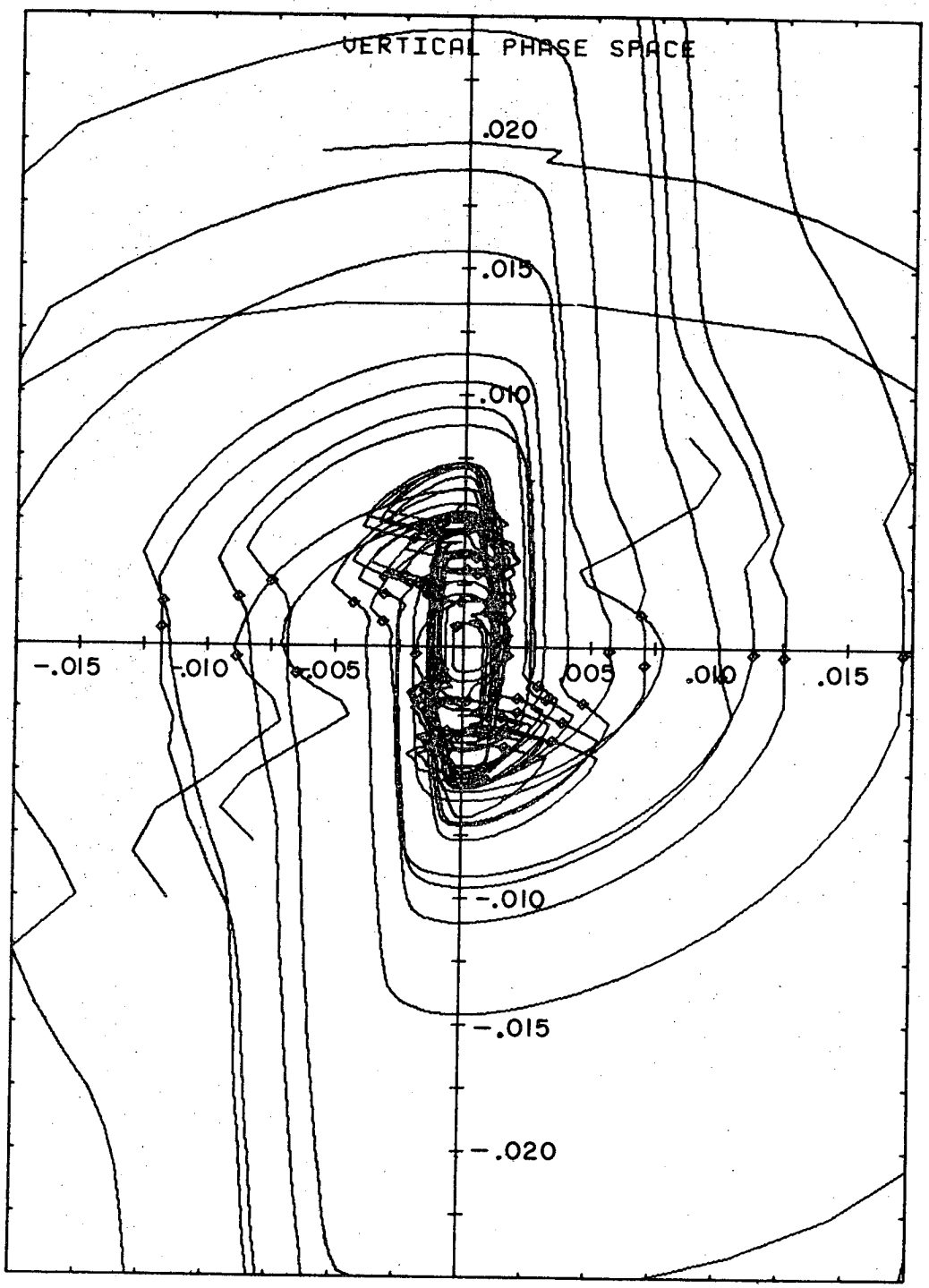

XBL706-3160

Fig. 7. Vertical phase space motion calculated by numerical integration of equations of motion in measured magnetic field. ◇ indicates azimuth of 116 deg, center of regeneration.

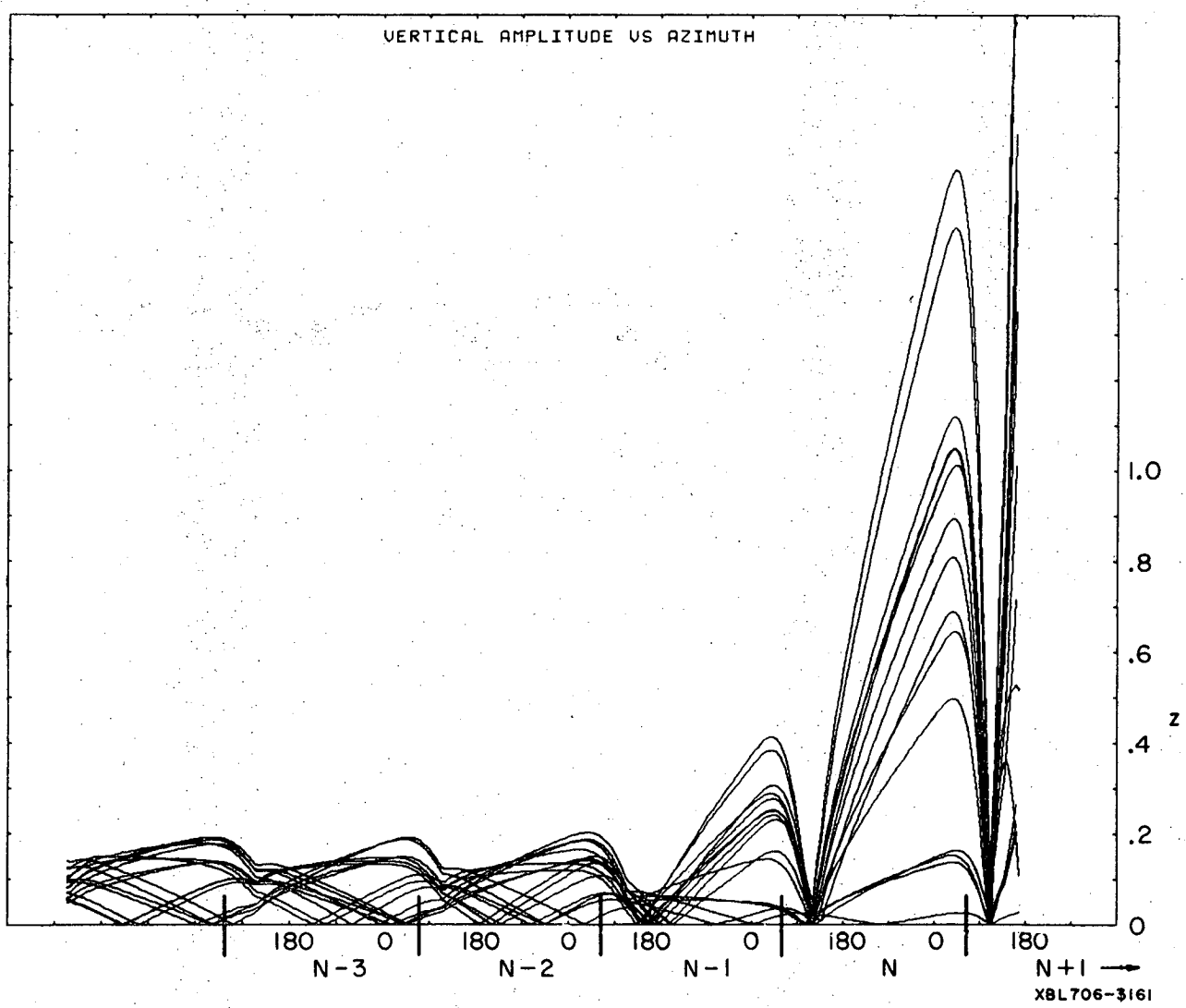

Fig. 8. Vertical amplitude of typical particle as function of azimuth for last four revolutions during regeneration.

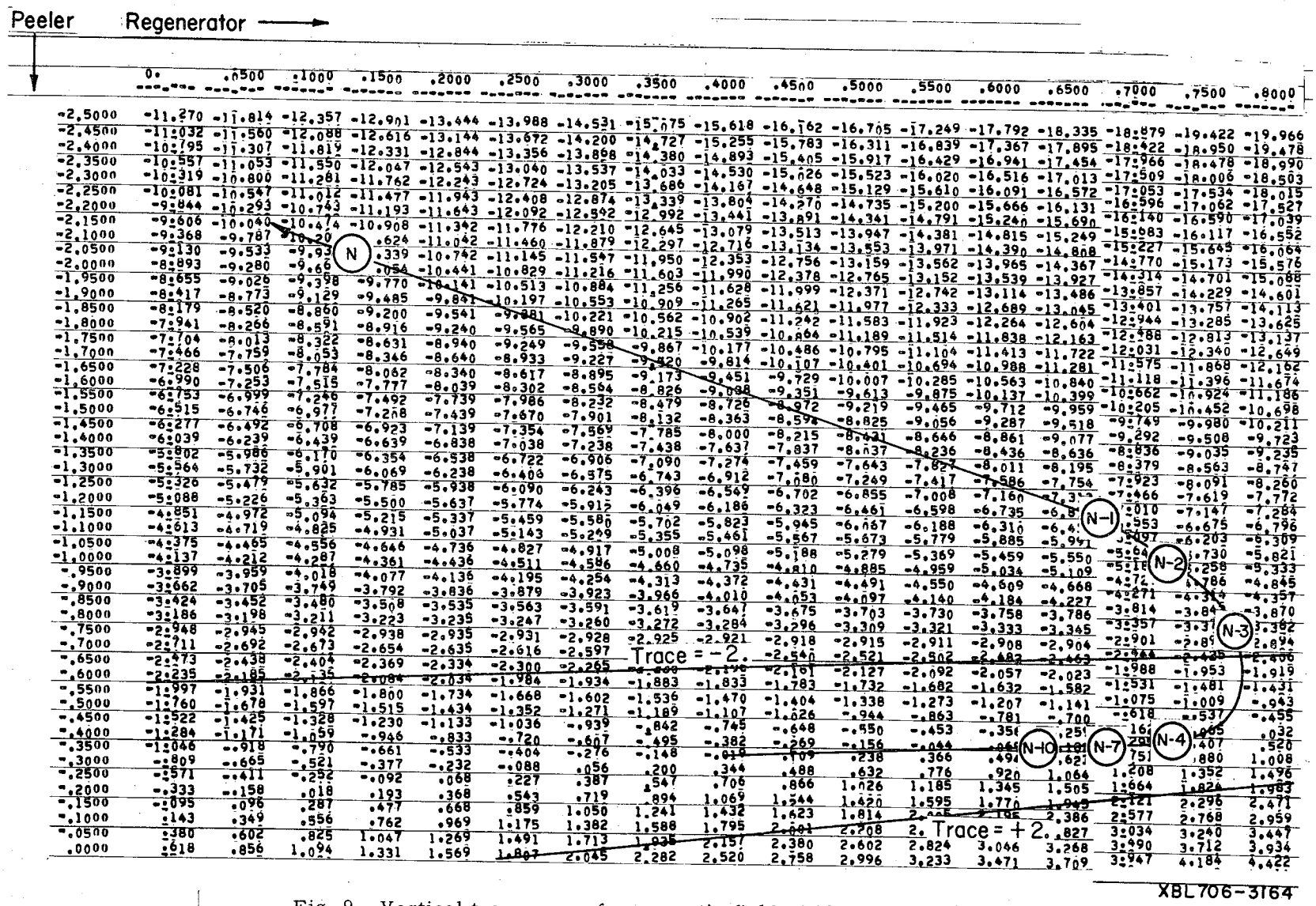

XBL706-3164

Fig. 9. Vertical trace space for magnetic field of 184-inch cyclotron, showing vertical stability limits and path taken by a typical particle undergoing regeneration. Note vertical instability on turns N-2, N-1, and N.

Peeler ↓ Regenerator →

	0.	.0500	.1000	.1500	.2000	.2500	.3000	.3500	.4000	.4500	.5000	.5500	.6000	.6500	.7000	.7500	.8000
-2.5000	1.665	1.800	1.936	2.072	2.208	2.344	2.480	2.616	2.752	2.888	3.024	3.159	3.295	3.431	3.567	3.703	3.839
-2.4500	1.671	1.804	1.938	2.071	2.204	2.337	2.471	2.604	2.737	2.871	3.004	3.137	3.271	3.404	3.537	3.671	3.804
-2.4000	1.677	1.808	1.939	2.069	2.200	2.331	2.462	2.592	2.723	2.854	2.985	3.115	3.246	3.377	3.507	3.638	3.769
-2.3500	1.684	1.812	1.940	2.068	2.196	2.324	2.453	2.581	2.709	2.837	2.965	3.093	3.221	3.349	3.478	3.606	3.734
-2.3000	1.690	1.816	1.941	2.067	2.192	2.318	2.443	2.569	2.694	2.820	2.946	3.071	3.197	3.322	3.448	3.573	3.699
-2.2500	1.696	1.819	1.942	2.065	2.188	2.311	2.434	2.557	2.680	2.803	2.926	3.049	3.172	3.295	3.418	3.541	3.664
-2.2000	1.703	1.823	1.944	2.064	2.184	2.305	2.425	2.545	2.666	2.786	2.907	3.027	3.147	3.268	3.388	3.508	3.629
-2.1500	1.709	1.827	1.945	2.063	2.180	2.298	2.416	2.534	2.651	2.769	2.887	3.005	3.123	3.240	3.358	3.476	3.594
-2.1000	1.716	1.831	1.946	2.061	2.176	2.292	2.407	2.522	2.637	2.752	2.868	2.983	3.098	3.213	3.328	3.443	3.559
-2.0500	1.722	1.835	1.947	2.060	2.172	2.285	2.398	2.510	2.623	2.735	2.848	2.961	3.073	3.186	3.298	3.411	3.524
-2.0000	1.728	1.838	1.948	2.058	2.168	2.278	2.388	2.498	2.608	2.718	2.828	2.938	3.049	3.159	3.269	3.379	3.489
-1.9500	1.735	1.842	1.950	2.057	2.164	2.272	2.379	2.487	2.594	2.702	2.809	2.916	3.024	3.131	3.239	3.346	3.453
-1.9000	1.741	1.846	1.951	2.056	2.161	2.265	2.370	2.475	2.580	2.685	2.789	2.894	2.999	3.104	3.209	3.314	3.418
-1.8500	1.748	1.850	1.952	2.054	2.157	2.259	2.361	2.463	2.566	2.668	2.770	2.872	2.974	3.077	3.179	3.281	3.383
-1.8000	1.754	1.854	1.953	2.053	2.153	2.252	2.352	2.452	2.551	2.651	2.750	2.850	2.950	3.049	3.149	3.249	3.348
-1.7500	1.760	1.857	1.955	2.052	2.149	2.246	2.343	2.440	2.537	2.634	2.731	2.828	2.925	3.022	3.119	3.216	3.313
-1.7000	1.767	1.861	1.956	2.050	2.145	2.239	2.334	2.428	2.523	2.617	2.711	2.806	2.900	2.995	3.089	3.184	3.278
-1.6500	1.773	1.865	1.957	2.049	2.141	2.233	2.324	2.416	2.508	2.600	2.692	2.784	2.876	2.968	3.059	3.151	3.243
-1.6000	1.780	1.869	1.958	2.047	2.137	2.226	2.315	2.405	2.494	2.583	2.672	2.762	2.851	2.940	3.030	3.119	3.208
-1.5500	1.786	1.873	1.959	2.046	2.133	2.219	2.306	2.393	2.480	2.566	2.653	2.740	2.826	2.913	3.000	3.086	3.173
-1.5000	1.792	1.876	1.961	2.045	2.129	2.213	2.297	2.381	2.465	2.549	2.633	2.718	2.802	2.886	2.970	3.054	3.138
-1.4500	1.799	1.880	1.962	2.043	2.125	2.206	2.288	2.369	2.451	2.532	2.614	2.695	2.777	2.858	2.940	3.021	3.103
-1.4000	1.805	1.884	1.963	2.042	2.121	2.200	2.279	2.358	2.437	2.515	2.594	2.673	2.752	2.831	2.910	2.989	3.068
-1.3500	1.812	1.888	1.964	2.041	2.117	2.193	2.270	2.346	2.422	2.499	2.575	2.651	2.728	2.804	2.880	2.957	3.033
-1.3000	1.818	1.892	1.965	2.039	2.113	2.187	2.260	2.334	2.408	2.482	2.555	2.629	2.703	2.777	2.850	2.924	2.998
-1.2500	1.824	1.896	1.967	2.038	2.109	2.180	2.251	2.322	2.394	2.465	2.536	2.607	2.678	2.749	2.820	2.892	2.963
-1.2000	1.831	1.899	1.968	2.036	2.105	2.174	2.242	2.311	2.379	2.448	2.516	2.585	2.653	2.722	2.791	2.859	2.928
-1.1500	1.837	1.903	1.969	2.035	2.101	2.167	2.233	2.299	2.365	2.431	2.497	2.563	2.629	2.695	2.761	2.827	2.893
-1.1000	1.844	1.907	1.970	2.034	2.097	2.160	2.224	2.287	2.351	2.414	2.477	2.541	2.604	2.667	2.731	2.794	2.858
-1.0500	1.850	1.911	1.972	2.032	2.093	2.154	2.215	2.275	2.336	2.397	2.458	2.519	2.579	2.640	2.701	2.762	2.823
-1.0000	1.856	1.915	1.973	2.031	2.089	2.147	2.206	2.264	2.322	2.380	2.438	2.497	2.555	2.613	2.671	2.729	2.788
-.9500	1.863	1.918	1.974	2.030	2.085	2.141	2.196	2.252	2.308	2.363	2.419	2.474	2.530	2.586	2.641	2.697	2.752
-.9000	1.869	1.922	1.975	2.028	2.081	2.134	2.187	2.240	2.293	2.346	2.399	2.452	2.505	2.558	2.611	2.664	2.717
-.8500	1.876	1.926	1.976	2.027	2.077	2.128	2.178	2.229	2.279	2.329	2.380	2.430	2.481	2.531	2.582	2.632	2.682
-.8000	1.882	1.930	1.978	2.025	2.073	2.121	2.169	2.217	2.265	2.312	2.360	2.408	2.456	2.504	2.552	2.599	2.647
-.7500	1.888	1.934	1.979	2.024	2.069	2.115	2.160	2.205	2.250	2.296	2.341	2.386	2.431	2.477	2.522	2.567	2.612
-.7000	1.895	1.937	1.980	2.023	2.065	2.108	2.151	2.193	2.239	2.279	2.321	2.364	2.407	2.449	2.492	2.535	2.577
-.6500	1.901	1.941	1.981	2.021	2.061	2.101	2.142	2.182	2.222	2.262	2.302	2.342	2.382	2.422	2.462	2.502	2.542
-.6000	1.907	1.945	1.982	2.020	2.057	2.095	2.132	2.170	2.207	2.245	2.282	2.320	2.357	2.395	2.432	2.470	2.507
-.5500	1.914	1.949	1.984	2.019	2.053	2.088	2.123	2.158	2.193	2.228	2.263	2.298	2.333	2.367	2.402	2.437	2.472
-.5000	1.920	1.953	1.985	2.017	2.049	2.082	2.114	2.146	2.179	2.211	2.243	2.276	2.308	2.340	2.372	2.405	2.437
-.4500	1.927	1.956	1.986	2.016	2.046	2.075	2.105	2.135	2.164	2.194	2.224	2.253	2.283	2.313	2.342	2.372	2.402
-.4000	1.933	1.960	1.987	2.014	2.042	2.069	2.096	2.123	2.150	2.177	2.204	2.231	2.258	2.286	2.313	2.340	2.367
-.3500	1.939	1.964	1.989	2.013	2.038	2.062	2.087	2.111	2.136	2.160	2.185	2.209	2.234	2.258	2.283	2.307	2.332
-.3000	1.946	1.968	1.990	2.012	2.034	2.056	2.077	2.099	2.121	2.143	2.165	2.187	2.209	2.231	2.253	2.275	2.297
-.2500	1.952	1.972	1.991	2.010	2.030	2.049	2.068	2.088	2.107	2.126	2.146	2.165	2.184	2.204	2.223	2.242	2.262
-.2000	1.959	1.975	1.992	2.009	2.026	2.042	2.059	2.076	2.093	2.109	2.126	2.143	2.160	2.176	2.193	2.210	2.227
-.1500	1.965	1.979	1.993	2.008	2.022	2.036	2.050	2.064	2.078	2.093	2.107	2.121	2.135	2.149	2.163	2.178	2.192
-.1000	1.971	1.983	1.995	2.006	2.018	2.029	2.041	2.052	2.064	2.076	2.087	2.099	2.110	2.122	2.133	2.145	2.157
-.0500	1.978	1.987	1.996	2.005	2.014	2.023	2.032	2.041	2.050	2.059	2.068	2.077	2.086	2.095	2.104	2.113	2.122
.0000	1.984	1.991	1.997	2.003	2.010	2.016	2.023	2.029	2.035	2.042	2.048	2.055	2.061	2.067	2.074	2.080	2.087

N-1 N-2 N-3 N-4 N-10

XBL706-3165

Fig. 10. Radial trace space of 184-inch cyclotron, showing particle path taken by typical particle undergoing regeneration.

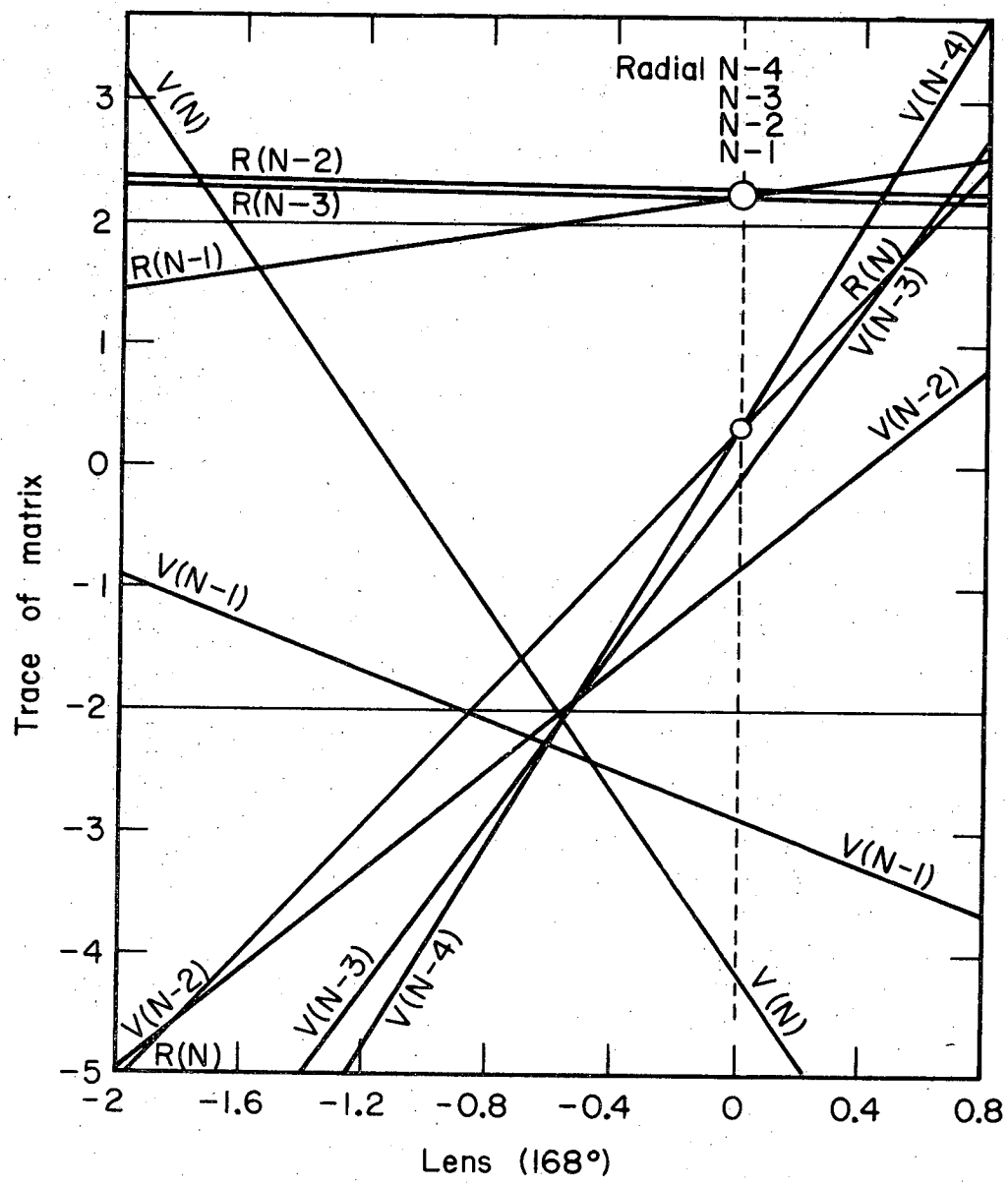

XBL706-3162

Fig. 11. Vertical and radial traces of transfer matrix as functions of lens strength at radial regeneration node for last five revolutions in 184-inch cyclotron. The matrices extend from 60, 116, and 168 to 60 deg and were calculated numerically by orbit integration in the existing magnetic field of the 184-inch cyclotron for typical 730-MeV protons. Here V(m) indicates vertical trace, m^{th} turn and R(m) indicates radial trace, m^{th} turn.

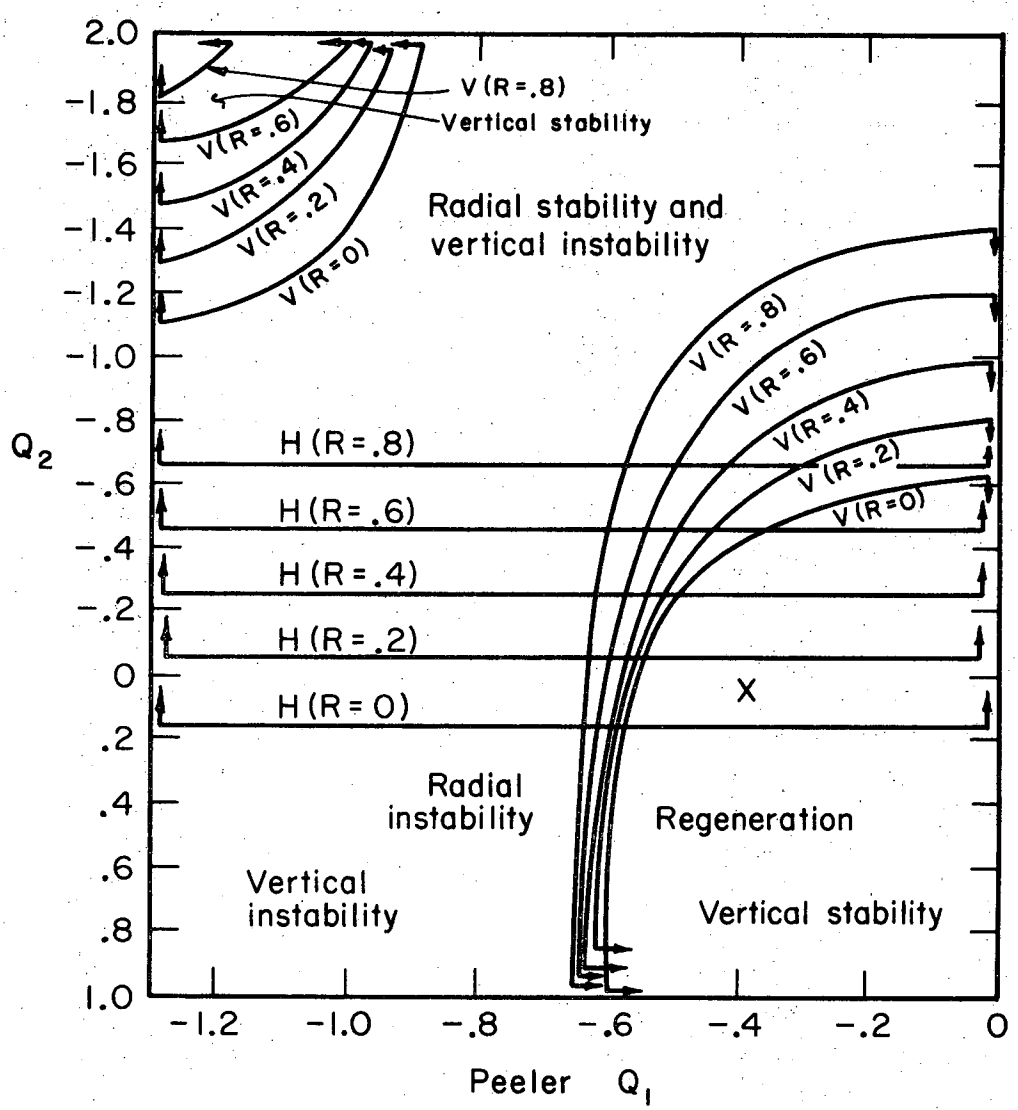

XBL 706-3163

Fig. 12. Stability diagram for magnetic bump beam stretcher. The lines are drawn for trace of matrix equal to 2.0 with arrows pointing in direction of trace less than 2.0. The curves are marked H for horizontal and V for vertical for regenerator strengths R as indicated. The point marked X is the current operating point where radial trace is greater than 2 and the vertical trace is less than 2, R = 0.6.

LEGAL NOTICE

This report was prepared as an account of Government sponsored work. Neither the United States, nor the Commission, nor any person acting on behalf of the Commission:

A. Makes any warranty or representation, expressed or implied, with respect to the accuracy, completeness, or usefulness of the information contained in this report, or that the use of any information, apparatus, method, or process disclosed in this report may not infringe privately owned rights; or

B. Assumes any liabilities with respect to the use of, or for damages resulting from the use of any information, apparatus, method, or process disclosed in this report.

As used in the above, "person acting on behalf of the Commission" includes any employee or contractor of the Commission, or employee of such contractor, to the extent that such employee or contractor of the Commission, or employee of such contractor prepares, disseminates, or provides access to, any information pursuant to his employment or contract with the Commission, or his employment with such contractor.

TECHNICAL INFORMATION DIVISION
LAWRENCE RADIATION LABORATORY
UNIVERSITY OF CALIFORNIA
BERKELEY, CALIFORNIA 94720